Flow Measurement and Instrumentation 109 (2026) 103215

Contents lists available at ScienceDirect

Flow Measurement and Instrumentation

journal homepage: www.elsevier.com/locate/flowmeasinst

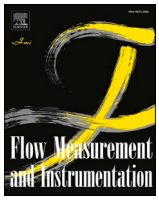

Research on vibration and noise reduction driving strategy of piezoelectric high-speed on/off valve based on second-order S-curve

Linfei Li [a], Yuwen Wang [a,b], Yuchuan Zhu [a,*]

[a] College of Mechanical and Electrical Engineering, Nanjing University of Aeronautics and Astronautics, Nanjing, 210016, China
[b] Nanjing Chenguang Group Industrial Co., Ltd., Nanjing, 210006, China

ARTICLE INFO

Keywords:
Piezoelectric high-speed on/off valve (PHSV)
Electromagnetic noise
Mechanical noise
Vibration and noise reduction pulse width modulation (VNR-PWM)
Soft landing

ABSTRACT

The piezoelectric high-speed on/off valve (PHSV) encounters two primary challenges under high-frequency pulse width modulation (PWM) driving conditions: electromagnetic noise resulting from the high-frequency charging and discharging of piezoelectric materials, and mechanical noise arising from the rapid, high-frequency impact between the valve spool and the valve seat. In order to solve this problem, this study proposes a vibration and noise reduction pulse width modulation (VNR-PWM) strategy based on second-order S-curve, aiming at realizing the soft-start and soft landing of the spool by optimizing the variation rules of the rising and falling curves in the PWM excitation voltage signal of the PHSV. The optimal parameter combinations of delay time T_0 and acceleration time t_{acc} in the VNR-PWM strategy are determined through simulation analysis. A prototype was developed, and the valve spool displacement, vibration noise and vibration acceleration experiments are carried out on the experimental platform to verify the performance of the VNR-PWM strategy. The vibration and noise experiments show that the opening and closing noise of the high-speed on/off valve is 70 dB and 80 dB respectively under the 0.25 Hz and 200 Hz VNR-PWM driving strategies. Compared with the traditional PWM driving strategy, the opening and closing noise is reduced by 12.5% and 16.3%, respectively. The acceleration test of the valve block shows that under the VNR-PWM drive strategy, the vibration acceleration of the valve block is reduced from 1130 m/s^2 to 265 m/s^2 (closing process) and 570 m/s^2 to 170 m/s^2 (opening process), with a decrease of about 76.5% and 70.2%.

1. Introduction

As the key core component of digital hydraulic technology, the dynamic characteristics of high-speed on/off valve have a direct impact on the performance of digital hydraulic components and even the whole system [1–3]. In order to achieve high flow resolution, zero leakage and wide duty cycle, both academia and industry research has focused on improving the dynamic response speed of high-speed on/off valve, particularly those employing ball and conical spool designs [4–6]. However, as the dynamic response speed of high-speed on/off valve increases, it inevitably results in high-frequency opening and closing of the valve spool, causing it to strike the valve seat at extremely high speeds. This leads to high-frequency impact noise and accelerates metal fatigue wear. This not only compromises the comfort of the working environment but also directly impacts the flow coefficient of the valve port and leakage characteristics, significantly shortening the service life of the high-speed on/off valve [7]. This contradicts the current trend toward developing hydraulic components with longer lifespans and higher reliability. Therefore, it is of great significance to study the vibration and noise reduction methods of the high-speed on/off valve.

In the research of vibration and noise reduction driving methods, some foreign scholars have achieved shock absorption and noise reduction through structural optimization. Amini et al.proposed a new configuration of a 60° conical spool and a rear seat gas pressure reducing valve, which reduced the noise by 12 dB [8]. Youn C.developed a pressure reducing valve with a radial slit throttling structure, and the experimental results show that the noise level is reduced by about 40 dB [9]. Borg et al. proposed an injector mount installation scheme, which reduced the noise of each characteristic frequency band of the gasoline direct injection system by 2 to 6 dB [10]. Lilia Badykova et al. installed a muffler at the outlet of the pressure reducing valve to reduce the working noise [11].

On the other hand, a large number of foreign scholars have achieved shock absorption and noise reduction through control strategies.

* Corresponding author.
E-mail address: meeyczhu@nuaa.edu.cn (Y. Zhu).

https://doi.org/10.1016/j.flowmeasinst.2026.103215
Received 21 May 2025; Received in revised form 6 January 2026; Accepted 21 January 2026
Available online 4 February 2026

Peterson et al. proposed an extreme value optimization controller based on the theory of impact sound intensity [12]. The controller employed the eddy current sensor to collect the displacement signal of the solenoid valve in real time. A velocity closed-loop control system was proposed, successfully achieving optimized control over the landing speed of the valve spool. Reuter et al. realized the smooth contact control of the spool trajectory by using the backstepping control strategy [13]. Tsai et al. proposed a adaptive feedforward approximation algorithm, which has good soft landing optimization ability, strong anti-disturbance robustness and high computational efficiency [14]. Glück et al. designed a feedforward controller for the oft landing time optimization problem of fast switching solenoid valve, and experimentally validated the feasibility of the algorithm. [15]. Bernardo et al. proposed a force control algorithm combining feedforward and feedback sliding mode for the soft-landing control problem of the dual-magnet solenoid valve [16]. The simulation results show that the proposed control method still has good soft-landing effect under the condition of external force disturbance and friction change. Mercorelli et al. used the coil current signal to estimate the valve speed, and adopted the control strategy of PID controller combined with feedforward controller to compensate the fixed error, which realized the effective control of the valve speed [17].

At the same time, many Chinese scholars have made significant progress in the research of vibration and noise reduction driving strategies. Li et al. proposed a variable structure sliding mode PID control strategy to solve the challenges of parameter uncertainty and strong interference, and realized the soft-landing control of solenoid valve [18]. Huang et al. proposed a staged control strategy to mitigate the impact of engine solenoid valve opening and closing shocks: open-loop control was used during the initial and early transitional phases of the process, while a linear quadratic regulator (LQR) method was switched to in the later motion stages to precisely control the seating speed [19]. Deng et al. proposed an observer-based feedback control system to improve the service life of high-speed dot-matrix pulse jet generator. This control strategy achieves precise trajectory tracking of high-speed dot-ma trix pulse jet generator without a sensor, effectively reducing the impact velocity and vibration noise of the valve spool and valve seat [20]. In addition, Zhu et al. proposed a two-layer control strategy composed of a semi-active controller in the inner layer and a linear quadratic regulator integrated in the outer layer to realize the soft-landing control of the solenoid valve. The experimental results show that the contact speed of the spool is reduced by 75.8 % and the height of spring back is reduced by 80 % [21]. In addition, the generation mechanism of high-speed on/off valve noise is studied in depth. Huang Hui et al.analyzed the motion characteristics of high-speed on/off valves under the action of electro-magnetic-fluid-solid coupling, and found that under 3Mpa, mechanical noise was the dominant. When it is greater than 3Mpa, fluid noise plays a leading role [22–24]. Huang Qiufang explored the influence of driving parameters of high-speed on/off valve on vibration and noise. The experimental results show that the lower the driving frequency and the larger the duty cycle, the more serious the vibration noise of the high-speed on/off valve [25].

In summary, there are few studies on vibration reduction and noise control strategies for high-speed on/off valves. Furthermore, existing control strategies for hydraulic valves heavily rely on displacement sensors or highly realistic simulation models to achieve precise identification of spool displacement states. These approaches impose stringent requirements on installation space and model accuracy. Moreover, Most existing research employ complex control algorithms to achieve spool vibration and noise reduction, demanding higher computational capabilities from hardware. In view of the above problems, this study aims to explore and propose a vibration and noise reduction control strategy that is widely applicable and consumes minimal computational resources, without relying on displacement sensors or highly realistic simulation models.

The manuscript focuses on the piezoelectric high speed on/off valve (PHSV), a PWM drive strategy for vibration and noise reduction based on the second-order S-shaped curve is proposed to achieve vibration and noise reduction. First, the structure, operating principle, and mechanism of the vibration and noise reduction drive strategy for PHSVs are analyzed. Then, through theoretical modeling and simulation analysis, the impact of key structural parameters in vibration and noise reduction control strategies on the dynamic characteristics of the piezoelectric high speed on/off valve. Based on this, the optimal key structural parameters are determined. Finally, a test bench is built to experimentally verify the effectiveness of the proposed vibration and noise reduction drive strategy. These research results provide new ideas for improving the service life and reliability of high speed on/off valves.

2. The structure and working principle

The structure and key components of the piezoelectric high speed on/off valve are shown in Fig. 1. It can be seen that the piezoelectric high speed on/off valve is mainly composed of cover, anti-torsion gasket, shell, ring/square piezoelectric, disc spring, adjusting screw, push rod, valve body and spool. In this study, the radial stack axial nested new structure is innovatively introduced into the electro-mechanical converter, and the superposition of the output displacement of the square and ring piezoelectricity is realized by the sleeve. It has the advantages of high frequency response, large output force and large output displacement, which meets the application requirements of high-speed on/off valve electro-mechanical converter. In addition, the spool is designed with a cone-slide valve structure, ensuring zero leakage and excellent pressure resistance of the PHSV.

The piezoelectric high speed on/off valve has two working modes: opening mode and closing mode. In the open mode, the piezoelectric stack is excited by the driving voltage to generate output displacement and output force. When the output force is able to overcome the spring force of the preloaded and reset disc springs as well as the obstruction force during the spool movement, the spool moves under the action of the output lever, allowing the inlet P to communicate with the outlet A, and the hydraulic fluid to flow through the cone-slip spool. On the contrary, the piezoelectric stack is not excited by the voltage in the closed mode, and the cone-slide valve spool is closely attached to the throttle valve seat under the combined action of the spring force of the preloaded disc spring and the reset disc spring. The inlet P and outlet A

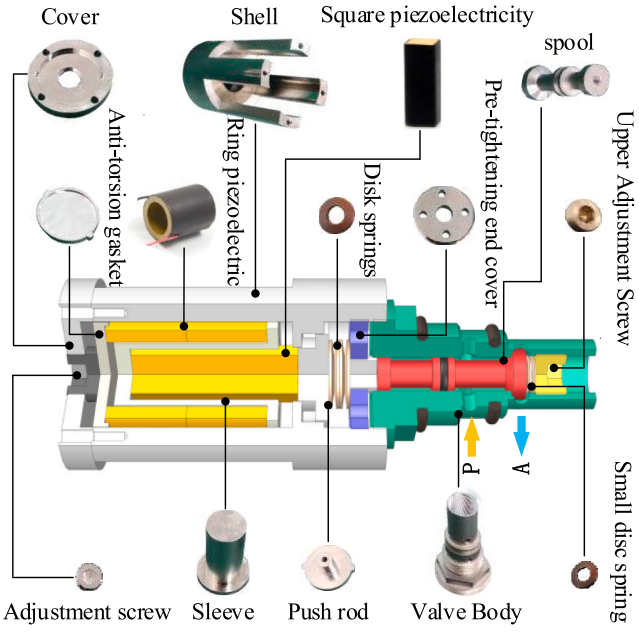

Fig. 1. Structure and key components of piezoelectric high speed on/off.

are effectively isolated, preventing hydraulic fluid from passing through the cone-slide valve.

3. Mathematical modeling

3.1. Piezoelectric stack motor converter

As shown in Fig. 2, the relationship curve between the output displacement and the output force of the piezoelectric stack motor converter under different supply voltages is described. This curve reflects the most critical output characteristic of the piezoelectric stack motor converter, namely, the correlation between the output displacement and the output force.

As shown in Fig. 2, there is a distinct linear correlation between the output force and the output displacement of the piezoelectric stack under different driving voltages. The relationship between the effective output force F_p and the output displacement x_p of the piezoelectric stack motor converter can be mathematically represented as:

$$F_p = K_T n d_{33} U - K_T x_p \tag{1}$$

in which n is the number of stacks, d_{33} is the piezoelectric coefficient, and U is the driving voltage, and K_T is the stiffness of the piezoelectric stack, which can be calculated by the following formula:

$$K_T = \frac{E_p A_p}{L_p} \tag{2}$$

Which E_p is the stiffness of the piezoelectric stack, A_p is the cross-sectional area of the stack material, and L_p is the total length of the piezoelectric stack.

Therefore, the output force F_{p1}, excitation voltage U and output displacement x_1 of the ring piezoelectric stack can be expressed as:

$$F_{p1} = K_{Tr} n_r d_{33} U - K_{Tr} x_1 \tag{3}$$

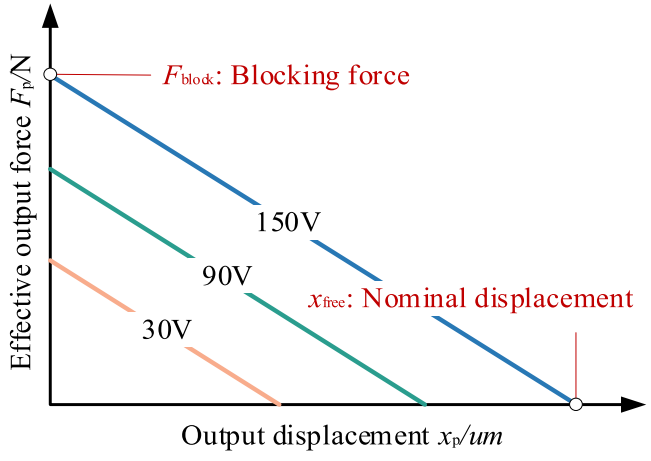

Fig. 2. Force-displacement output of piezoelectric stack motor converter under different supply voltage(F_{block}: blocking force, x_{free}: nominal displacement).

where K_{Tr} is the stiffness of the ring piezoelectric stack, n_r is the number of ring piezoelectric stack.

The square piezoelectric output force F_{p2}, excitation voltage U and output displacement x_2 can be expressed as:

$$F_{p2} = K_{Ts} n d_{33} U - K_{Ts} x_2 \tag{4}$$

where K_{Ts} is the stiffness of the ring piezoelectric stack, n_s is the number of square piezoelectric stack.

3.2. Dynamics modeling

According to the structure and working principle of the PHSV, the dynamic diagram of the PHSV is shown in Fig. 3. In the study, the elastic deformation is neglected because the spring stiffness of the sleeve, the output rod and the valve spool is much larger than that of the preloaded disc spring and the reset spring. According to Fig. 3, the dynamic mathematical model of the PHSV can be expressed as:

$$\begin{cases} F_{p1} - F_{p2} = \left(\frac{1}{3}m_1 + m_2\right)\ddot{x}_1 + c_3\dot{x}_1 \\ F_{p2} - F_s - F_t = \left(\frac{1}{3}m_3 + m_4 + m_5\right)(\ddot{x}_1 + \ddot{x}_2) + (c_1 + c_2)(\dot{x}_1 + \dot{x}_2) + (k_1 + k_2)(x_1 + x_2) \end{cases} \tag{5}$$

where x_1 is the output displacement of ring piezoelectric, x_2 is the output displacement of square piezoelectric, F_{p1} is the ring piezoelectric effective output force, F_{p2} is the effective output force of square piezoelectric, F_s and F_t are the steady-state and transient hydrodynamic forces of the valve spool, m_1 is the mass of ring piezoelectric, m_2 is the mass of sleeve, m_3 is the mass of square piezoelectric, m_4 is the mass of output rod, m_5 is the mass of valve spool, k_1 is the stiffness of the preloaded disc spring, k_2 is the stiffness of the reset disc spring, c_1, c_2 and c_3 are the kinematic viscous damping coefficients of the output rod, valve spool and sleeve, respectively.

3.3. Flow force of the spool

The spool of the PHSV is a cone-slide valve structure, where the slide valve structure serves to balance hydraulic pressure and provide guidance. The cone valve structure is responsible for controlling the fluid flow, and a schematic of the cone valve structure is shown in Fig. 4.

The flow area A_p of the cone valve can be expressed as:

$$A_p = \pi x_p \sin\alpha\left(d_s - x_p \sin\alpha \cos\alpha\right) \tag{6}$$

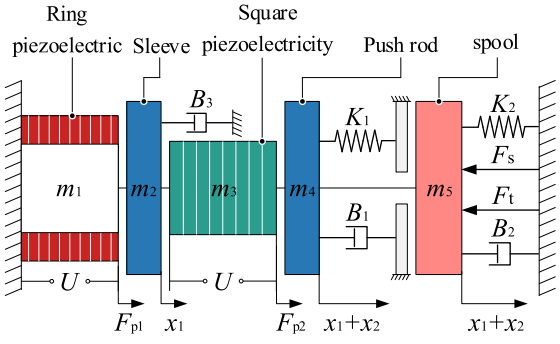

Fig. 3. Force balance diagram of PHSV.

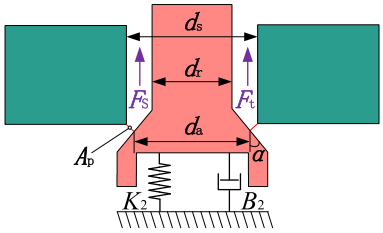

Fig. 4. Schematic diagram of the valve spool structure.

where x_p is the cone valve opening, which can be obtained by $x_p = x_1 + x_2$, α is the half cone angle of the valve spool, and d_s is the cone valve diameter.

During hydraulic oil flow through the valve spool, hydrodynamic forces are generated on the valve component. These forces can be categorized into two distinct types based on their temporal characteristics: transient hydrodynamic force and steady-state hydrodynamic force. The steady-state hydrodynamic force F_t acting on the valve spool can be mathematically described as:

$$F_t = 2C_v C_d A_p \Delta p \cos\theta \tag{7}$$

where C_v is the velocity coefficient and θ is the jet angle.

The transient flow force F_s of the poppet valve can be expressed as:

$$F_s = C_d A_p L\sqrt{2\Delta p\rho}\dot{x}_p \tag{8}$$

where L is the actual flow length of the fluid in the valve chamber, and ρ is the density of the oil.

4. Vibration and noise reduction PWM control strategy (VNR-PWM)

Fig. 5 shows the schematic diagram of the displacement and velocity variations of the PHSV spool under conventional PWM and VNR-PWM driving voltages. As shown in the figure, the conventional PWM drive voltage primarily consists of three components: the rising edge, the stabilization section, and the falling edge. Among these, the rapid changes in driving voltage at the rising and falling edges cause the piezoelectric stack to undergo rapid charging and discharging, which drives the valve spool to move quickly. This results in a violent impact when the valve spool contacts the valve seat. This impact is a key factor contributing to the strong electromagnetic and mechanical noise produced by PHSV, as well as their shortened service life.

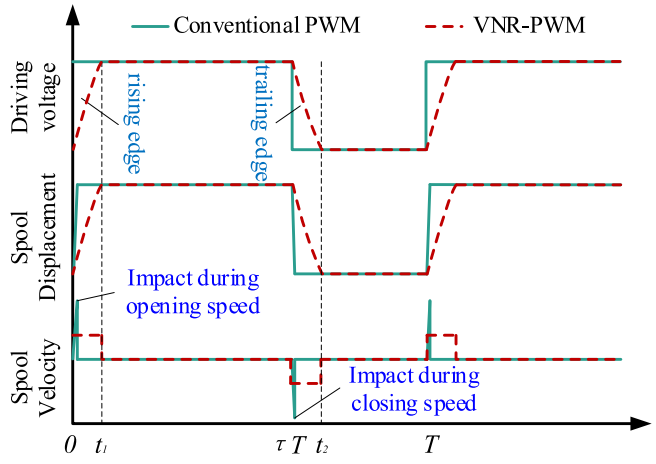

Fig. 5. The variation of spool displacement and velocity of PHSV under different control strategies.

To address these issues, it is proposed to optimize the design of the rising and falling edge curves of the conventional PWM driving voltage, without relying on additional sensors to monitor the spool's motion state. On the premise of sacrificing the dynamic performance of the PHSV, the noise level during the opening and closing of the spool is significantly reduced, and its service life is effectively extended.

At present, many scholars both domestically and internationally have designed various types of target trajectory design methods, which can be categorized according to the target trajectory: low-pass filtering curves, power function curves [26], second-order S-shaped curves [27], third-order S-shaped curves [28] and so on. The low-pass filtering curve refers to the target trajectory of the valve spool, which is the square wave curve after being processed by first-order low-pass filtering. Its mathematical expression is:

$$x_d(t) = \frac{1}{T}\exp\left(-\frac{t}{T}\right) \tag{9}$$

where T is the time constant, which determines the trajectory of the curve. The rise time of the curve is defined as the delay time, given by $T_0 = 4T$.

The expression for the power function curve is as follows:

$$x_d(t) = x_{max} - x_{max}\exp\left(-\frac{\eta t^2}{2}\right) \tag{10}$$

where x_{max} represents the maximum opening of the spool, and η is the trajectory control parameter. By adjusting η, the ideal trajectory can be achieved to ensure the spool moves at the desired speed. T_0 is the delay time of the curve.

The second-order S-shaped displacement curve is named according to the characteristics of its position trajectory obtained by two integrals. The acceleration expression of the curve is as follows:

$$a = \begin{cases} a_{max} & 0 < t < t_{acc} \\ 0 & t_{acc} < t < T_0 - t_{acc} \\ -a_{max} & T_0 - t_{acc} < t < T_0 \end{cases} \tag{11}$$

where a_{max} is the maximum acceleration of the second-order S-shaped curve, t_{acc} is the acceleration time, T_0 is the delay time of the curve, and velocity and displacement are the first-order and second-order integrals of acceleration a, respectively.

By referencing the typical target trajectory curve, driving voltage curves for vibration and noise reduction based on different function types have been generated, as shown in Fig. 6. In the low-pass filter curve, $T = 0.25$ ms and $T_0 = 1$ ms; In the power function curve, $\eta = -20000$; In the second-order S-shaped curve, $t_{acc} = 0.2$ ms and $T_0 = 1$ ms.

As shown in Fig. 6, within the same voltage response time, the maximum rate of voltage change of the low-pass filtering curve is 6.2×10^5 V/s, while that of the power function curve is 2.6×10^5 V/s. The maximum rates of voltage change for the second-order and third-order S-curves are similar, at 1.6×10^5 V/s and 1.8×10^5 V/s, respectively. To reduce vibration and noise in the PHSV, the change rate of the driving voltage should be smaller.

Considering both the implementation cost and effectiveness, the second-order S-shaped curve is applied to the rising and falling edges of the conventional PWM signal, thereby generating a vibration and noise reducing PWM signal. The speed of the spool opening and closing process is controlled, thereby reducing both the vibration noise and piezoelectric excitation noise of the PHSV.

The movement displacement of the spool in the PHSV follows a consistent trend with the driving voltage. This phenomenon is due to the strong linear correlation between the driving voltage of the piezoelectric stack and its output displacement. Therefore, in the follow-up study, a reverse approach will be adopted: first, the displacement, velocity, and acceleration parameters of the valve spool in the ideal state will be determined; then, the required piezoelectric stack driving voltage will

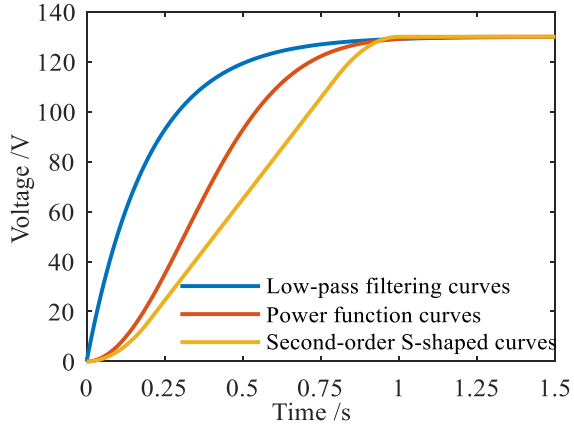

(a) Voltage

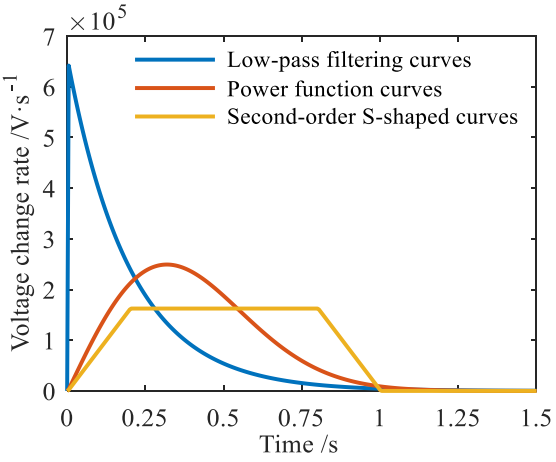

(b) Rate of change of voltage

Fig. 6. Voltage variation curves for different function types.

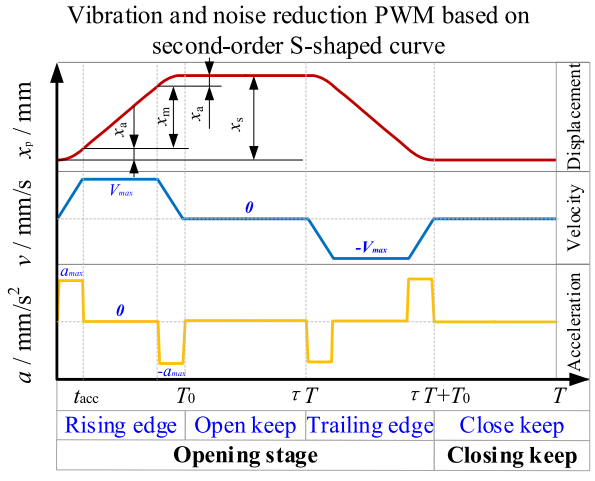

Fig. 7. Variation law of displacement, velocity and acceleration of PHSV by VNR-PWM.

be derived inversely.

As shown in Fig. 7, within a single working cycle, the movement process of the spool can be divided into four stages: rising, opening holding, descending, and closing holding. Moreover, the displacement change trends during the rising and descending stages are symmetrical.

In the rising stage, during the period from 0 to t_{acc}, the spool accelerates to the maximum speed Vmax with the maximum acceleration a_{max}, and the displacement gradually increases to x_a. In the range of t_{acc} to T_0-t_{acc}, the spool moves at a constant speed V_{max} to complete the displacement x_m. In the stage from T_0-t_{acc} to T_0, the spool decelerates at the maximum deceleration $-a_{max}$ to zero, achieving slow deceleration and completing the displacement x_a. T_0 realize the S-shaped curve characteristics of the

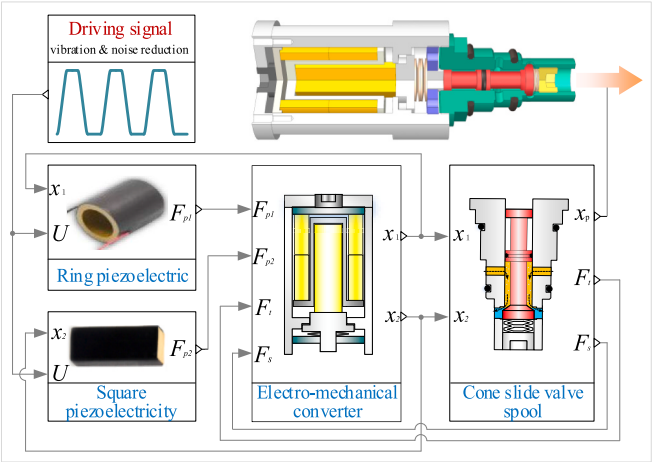

Fig. 8. Simulation model of PHSV.

Table 1
Parameter table of simulation model of PHSV.

Name	Sign	Value
Half cone angle of cone slide valve/°	θ	60
Flow coefficient	C_d	0.4
Oil density/Kg/m^3	ρ	870
Velocity factor	C_v	0.9
Pre-tightening disc spring stiffness/N/mm	k_1	466
Stiffness of reset disc spring/N/mm	k_2	206
Ring piezoelectric stack mass/Kg	m_1	0.07
Sleeve quality/Kg	m_2	0.023
Square piezoelectric stack mass/Kg	m_3	0.015
Output rod mass/Kg	m_4	0.04
Spool mass/Kg	m_5	0.035
Viscous damping coefficient of output rod/N/(m/s)	C_1	5000
Viscous damping coefficient of valve spool/N/(m/s)	C_2	4000
Viscous damping coefficient of valve sleeve/N/(m/s)	C_3	4000

spool motion trajectory, the parameters x_m, x_s, t_{acc}, V_{max} and T_m need to satisfy the following formulas:

$$\begin{cases} x_m = V_{max} T_m \\ x_s = x_a + x_m + x_a \\ t_{acc} = \dfrac{V_{max}}{a_{max}} \\ T_m = \dfrac{x_s - 2x_a}{V_{max}} \end{cases} \tag{12}$$

When designing the S-shaped curve, the total displacement x_s of the spool movement, the displacement x_a of the uniform acceleration stage and the maximum speed V_{max} of the spool can be determined first. The acceleration time t_{acc} and delay time T_0 ($T_0 = 2{*}t_{acc} + T_m$) can be obtained by using Formula 12, and then the expression of the spool displacement in a working cycle can be obtained by using Formula 13:

$$x = \begin{cases} \dfrac{1}{2} a_{max} t^2 & 0 < t \le t_{acc} \\ \dfrac{1}{2} a_{max} {t_{acc}}^2 + V_{max}(t - t_{acc}) & t_{acc} < t \le T_0 - t_{acc} \\ \dfrac{1}{2} a_{max} {t_{acc}}^2 + V_{max} T_m + V_{max}(t - T_m - t_{acc}) - \dfrac{1}{2} a_{max}(t - T_m - t_{acc})^2 & T_0 - t_{acc} < t \le T_0 \\ a_{max} t_{acc}^2 + V_{max} T_m & T_0 < t \le \tau T \\ a_{max} t_{acc}^2 + V_{max} T_m - \dfrac{1}{2} a_{max}(t + T_0 - \tau T)^2 & \tau T < t \le \tau T + t_{acc} \\ \dfrac{1}{2} a_{max} t_{acc}^2 + V_{max} T_m - V_{max}(t - \tau T + t_{acc} + T_m) & \tau T + t_{acc} < t \le \tau T + T_0 - t_{acc} \\ \dfrac{1}{2} a_{max} t_{acc}^2 - {V_{max}}^{*}(t + t_{acc} - \tau T) + \dfrac{1}{2} a_{max}(t + t_{acc} - \tau T)^2 & \tau T + T_0 - t_{acc} < t \le \tau T + T_0 \\ 0 & \tau T + T_0 < t \le T \end{cases} \tag{13}$$

5. Simulation modeling and simulation analysis

5.1. Simulation modeling

According to Equations (3)–(13), a simulation model of the PHSV is established by MATLAB, as shown in Fig. 8. It can be seen that the simulation model is mainly composed of five modules: drive signal, ring piezoelectric, square piezoelectric, electro-mechanical converter and cone slide valve spool.

According to the structural characteristics and functional parameters of the PHSV, the key parameters in the model are set. Table 1 shows the set values of some key parameters in the simulation model of PHSV.

5.2. Simulation analysis

The delay time T_0 and acceleration time t_{acc} are critical parameters in VNR-PWM based on the second-order S-curve. These parameters directly influence the valve spool's vibration and noise reduction performance as well as the dynamic response speed of its opening and closing. However, a trade-off exists between the spool's vibration and noise reduction effectiveness and its dynamic characteristics. Therefore, it is essential to examine the impact of delay time T_0 and acceleration time t_{acc} on the dynamic behavior of the spool and identify the optimal action times that achieve the best balance between the two factors.

(1) Delay time T_0

Fig. 9 shows the simulation results illustrating the influence of different delay times T_0 on the opening and closing characteristics of PHSV. During the simulation, the acceleration time t_{acc} of the PWM control strategy based on second-order S-curve vibration and noise reduction is set to $T_0/3$. As shown in the figure, it can be seen that the response time T_0 in the second-order S-curve has a greater influence on the displacement response of the PHSV. As the delay time T_0 increases, the displacement overshoot of the PHSV during the opening and closing process gradually decreases, and the opening and closing time of the valve spool gradually increases. Especially when $T_0 = 0.3$ ms, the displacement overshoot during the valve spool opening and closing process is particularly obvious.

In order to further analyze the influence of different delay time T_0 on the opening and closing characteristics of the PHSV, the opening and closing time of the valve spool under different delay time T_0 is extracted, and the results are shown in Fig. 10. As illustrated in the diagram, the closing time of the spool is longer than the opening time. The opening and closing time of the spool is proportional to the delay time. Therefore, the delay time T_0 should be appropriately selected based on the opening and closing time requirements of the piezoelectric high-speed switching valve.

(2) Acceleration time t_{acc}

Fig. 11 shows the simulation results illustrating the influence of

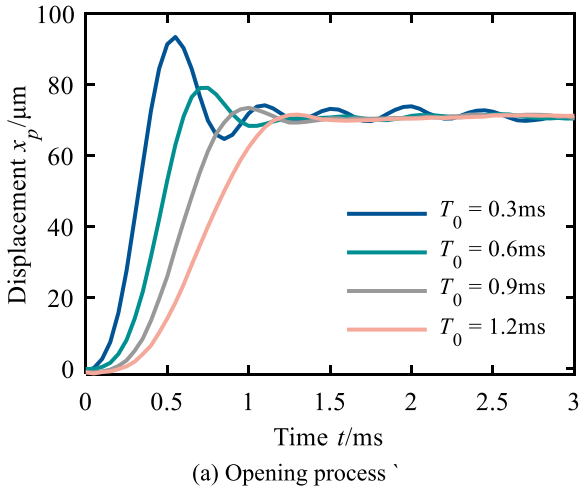

(a) Opening process `

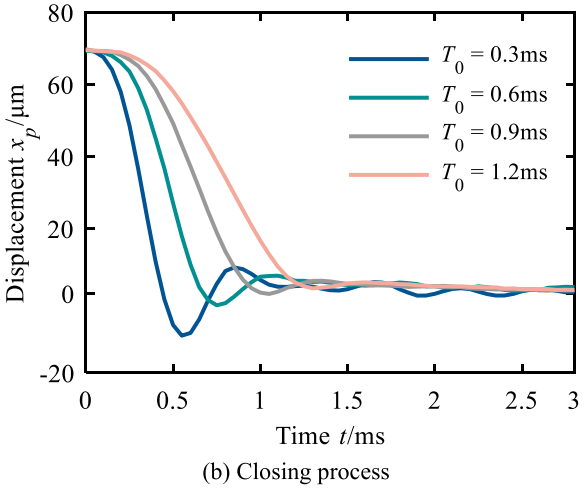

(b) Closing process

Fig. 9. Simulation results of dynamic response of PHSV displacement with different delay time T_0.

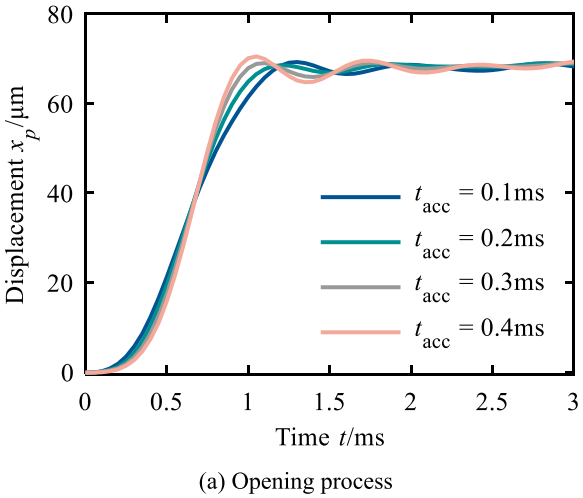

(a) Opening process

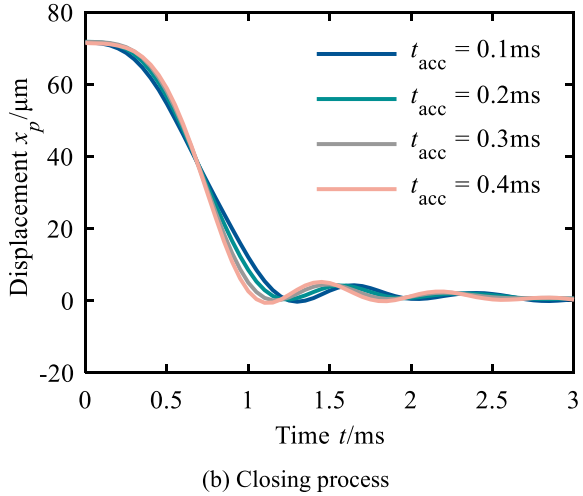

(b) Closing process

Fig. 11. Simulation results of dynamic response of actuator displacement with different acceleration time t_{acc}.

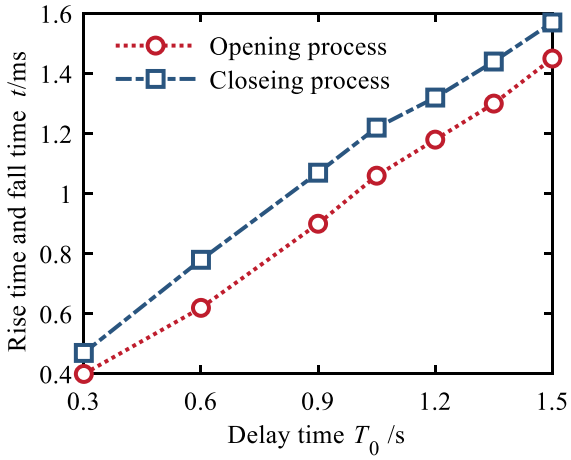

Fig. 10. Simulation results of rise time in actuator displacement response with different delay times T_0.

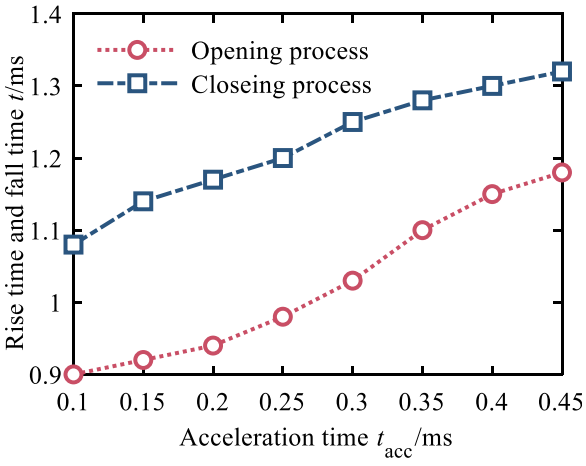

Fig. 12. Rise time results in actuator displacement response for different acceleration times t_{acc}.

different acceleration times t_{acc} on the opening and closing characteristics of PHSVs. During the simulation, the delay time T_0 of the PWM control strategy based on the second-order S-curve vibration and noise reduction is set to 1 ms. It can be seen from the diagram that the acceleration time t_{acc} in the second-order S-shaped curve has little effect on the opening and closing time of the PHSV. In addition, since the delay time in the second-order S-shaped curve is 1 ms, the displacement response of the PHSV at different acceleration times has only a small overshoot.

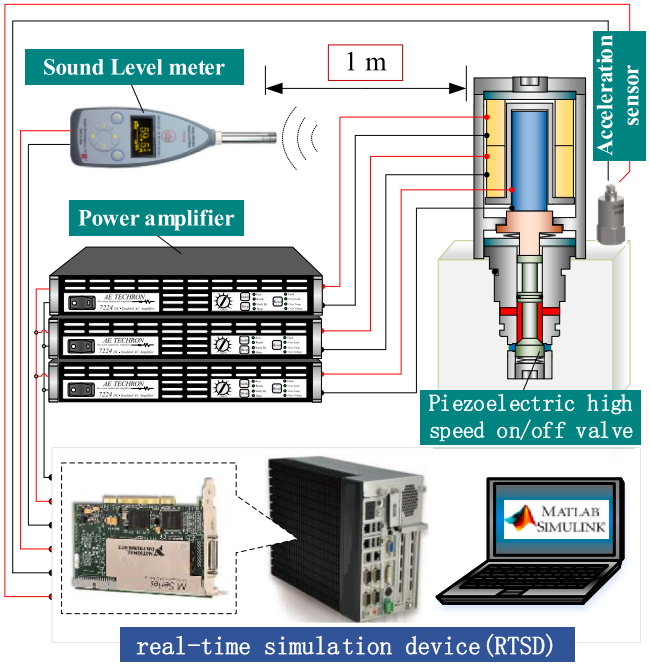

Fig. 13. Experimental principle of vibration and noise test of piezoelectric high speed on/off valve.

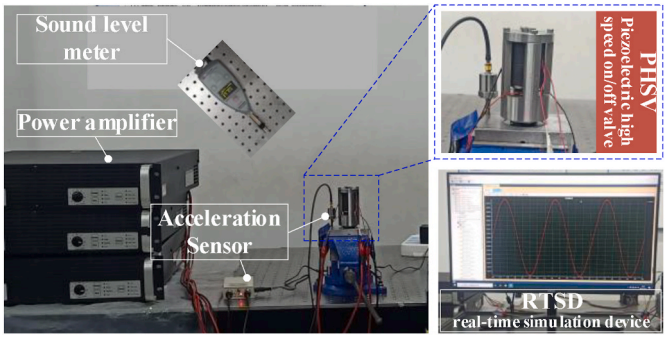

Fig. 14. Experimental physical diagram of vibration and noise test of PHSV.

Similarly, the opening and closing time of the PHSV for different acceleration times t_{acc} is shown in Fig. 12. From the figure, it can be seen that under the effect of VNR-PWM, the closing time of the valve is greater than the opening time. Additionally, the opening and closing time under different acceleration times is also different, but the overall variation range is small. When the acceleration time increases from 0.1 ms to 0.45 ms, the opening time of valve increases from 0.9 ms to 1.18 ms, and the closing time of valve increases from 1.18 ms to 1.42 ms. After analyzing, the reason for the kind of phenomenon is that different acceleration time t_{acc} has less effect on the trajectory of the second-order S-curve, and therefore its effect on the rise time of the displacement response of the actuator is also less.

Based on the simulation results of the above research, the delay time T_0 is set to 1 ms, and the acceleration time t_{acc} is set to $1/3*T_0$. Based on ensuring the dynamic response time of the PHSV, the vibration and noise of the PHSV are effectively reduced.

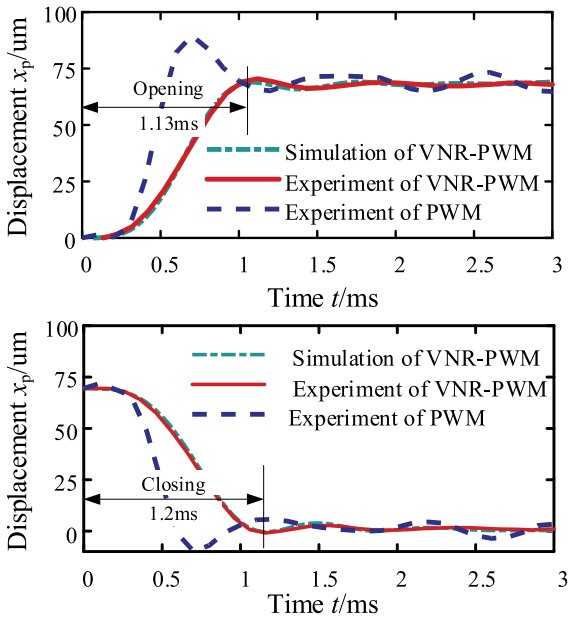

Fig. 15. Comparison of experimental and simulation results of spool displacement.

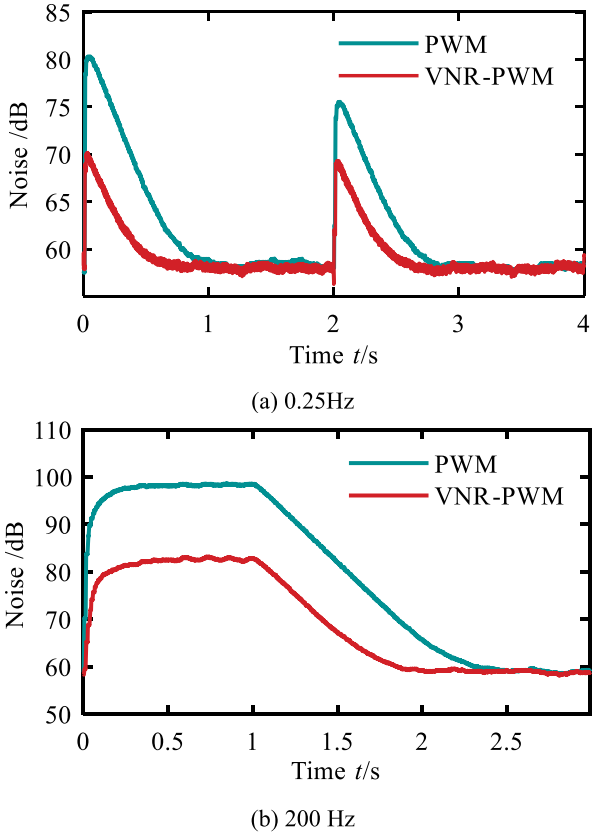

Fig. 16. Noise experimental comparison of conventional PWM and VNR-PWM strategy of PHSV.

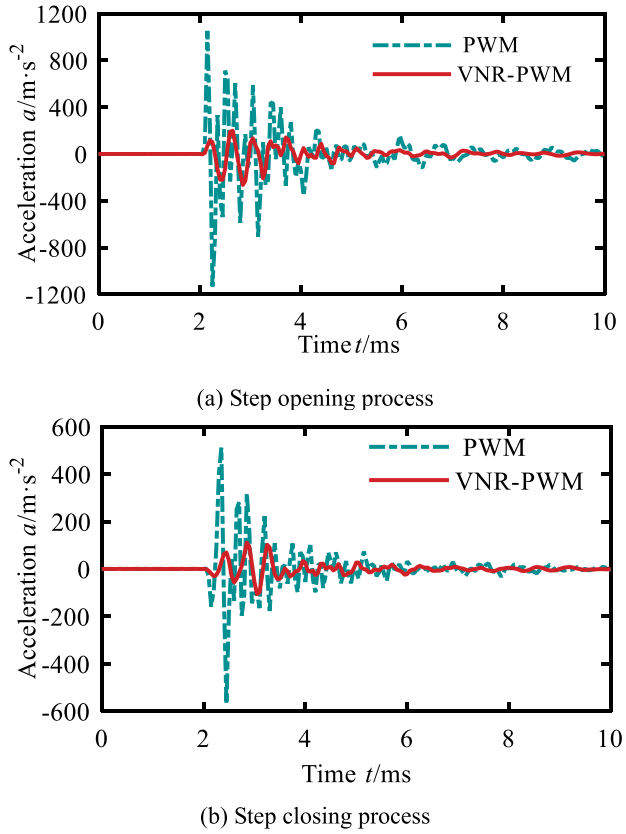

Fig. 17. Experimental results of the surface vibration acceleration of the valve block with no hydraulic fluid flow.

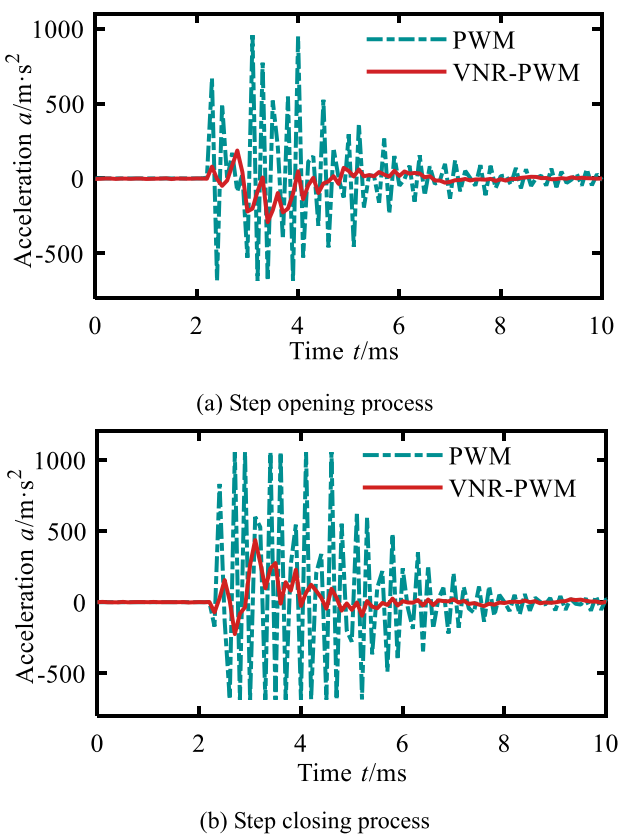

Fig. 18. Experimental results of the surface vibration acceleration of the valve block with hydraulic fluid flow.

6. Experimental verification

6.1. Experimental system composition and experimental principle

In order to verify the effectiveness of the VNR-PWM control strategy proposed in this study, it is necessary to build a PHSV test bench. As shown in Figs. 13 and 14, the experimental schematic diagram of the vibration and noise test of the PHSV and the physical schematic diagram are built respectively. The experimental platform is mainly composed of hardware-in-the-loop simulation system (Box-03), power amplifier (AETechron 7224), acceleration sensor (CA-YD-181), sound level meter (AWA5661) and other core components.

To generate the excitation voltage for the PHSV, the VNR-PWM based on S function is built by Simulink on the host computer. After binary encoding, the program is transmitted to the industrial control computer, which outputs the control signal to the power amplifier through its built-in acquisition card. The control signal is then amplified to meet the driving requirements of the PHSV. Furthermore, the acceleration sensor in the test bench is installed on the oil circuit block of the PHSV, and its installation direction is strictly consistent with the movement direction of the valve spool, so as to accurately evaluate the vibration generated during the opening and closing of the PHSV. In order to reduce the influence of the experimental device itself on the noise measurement, the measuring point of the sound level meter is set at a distance of 1m from the PHSV [29] to measure and record the noise level generated by the PHSV in real time.

6.2. Experimental result analysis

(1) Displacement Experiment

As shown in Fig. 15, the simulation and experimental results of the spool displacement are compared. Under the control strategy of VNR-PWM, the opening and closing time of the valve spool are 1.13 ms and 1.2 ms respectively. The simulation results are consistent with experimental data, which fully verifies the accuracy of the established simulation model. In addition, compared with the traditional PWM control strategy, the VNR-PWM control strategy significantly reduces the maximum overshoot of the spool and shortens its stabilization time. The experimental results verify the effectiveness of the proposed control strategy for VNR-PWM.

(2) Noise experiment

As shown in Fig. 16 (a), under the driving frequency of 0.25 Hz and the duty cycle of 0.5, the noise amplitude of the valve spool during opening and closing initially increases and then gradually decreases under both the conventional PWM drive and the vibration and noise-reduction PWM drive. Among them, the maximum noise of the high-speed on/off valve spool opening/closing under the conventional PWM drive is 80 dB and 75.5 dB respectively, while the maximum noise of the high-speed on/off valve spool opening/closing under the VNR-PWM drive is 70 dB. Compared with the conventional PWM drive signal, the maximum valve spool opening and closing noise amplitude under the VNR-PWM drive is reduced by 12.5% and 7.3% respectively, which verifies the effectiveness of the VNR-PWM drive strategy proposed in this paper.

From Fig. 16 (b), it can be seen that the noise of the opening and closing process of the high-speed on/off valve spool is a stable value at the driving frequency of 200 Hz and the duty cycle of 0.5, which is caused by the insufficient resolution of the sound pressure meter used in the experiment. Additionally, the opening and closing noise of the high-speed on/off valve spool is 98 dB and 82 dB (a reduction of approximately 16.3%) under the conventional PWM and VNR-PWM drive,

which is larger than the maximum opening and closing noise when the driving frequency is 0.25 Hz. And it is consistent with the above change rule of the opening and closing noise of the high-speed on/off valve and the frequency of the drive signal.

(3) Acceleration experiment

In order to further verify the effect of the proposed VNR-PWM control strategy, the surface vibration acceleration of the oil circuit block, designed for installing the PHSV, is studied under the step signal. As shown in Fig. 17, the experimental results of the valve block under the condition of no oil flow are presented.

As shown in Fig. 17(a), compared with the conventional PWM, the vibration acceleration of the hydraulic oil circuit block under the VNR-PWM control strategy is reduced from 1130 m/s2 to 265 m/s2, which is reduced by 76.5 %; As shown in Fig. 17 (b), during the closing process, the vibration acceleration of the valve block is reduced from 570 m/s^2 to 170 m/s^2, a decrease of 70.2%. This further demonstrates that the vibration and noise-reduction PWM effectively reduces the vibration of the PHSV.

Experimental results of the surface vibration acceleration of the valve block with hydraulic fluid flow are shown in Fig. 18. It can be seen from the figure that compared with the valve block without oil, the surface vibration acceleration of the valve block increases significantly and the duration increases. The reason for this phenomenon is that, under the condition with oil flow, the hydraulic circuit during the opening and closing process of the PHSV generates pressure shocks. These shocks are transmitted to the valve block and coupled with the vibration of the valve seat impacted by the spool.

However, it can still be clearly seen from the figure that compared with the PWM control strategy, the VNR-PWM control strategy still has a significant damping effect. During the opening and closing process of the spool, the vibration acceleration of the valve block is reduced by 70% and 58.6% respectively.

7. Conclusion

To address the issues of significant electromagnetic and mechanical noise, as well as the short service life of the piezoelectric high-speed switching valve, a VNR-PWM strategy based on a second-order S-curve is proposed. By precisely controlling the rise and fall rates of the driving voltage, smooth charging and discharging of the PHSV's motor converter are achieved, along with a soft landing of the valve spool. This method effectively controls the noise while ensuring the dynamic characteristics of the valve spool's opening and closing.

(1) The delay time T_0 in the VNR-PWM strategy is directly proportional to the spool's opening and closing time. The influence on the opening and closing time of the valve spool is negligible when the acceleration time t_{acc} changes within a certain range.
(2) The results of vibration and noise experiments demonstrate that, without compromising the dynamic performance of the spool's opening and closing, the opening and closing noise of the high-speed on/off valve is 70 dB and 80 dB respectively under the 0.25 Hz and 200 Hz damping and noise reduction PWM drive strategies. Compared with the conventional PWM drive strategy, the opening and closing noise is reduced by 12.5% and 16.3% respectively.
(3) The experimental results concerning the vibration acceleration of the valve block demonstrate that, when employing the VNR-PWM drive strategy, the vibration acceleration of the valve block decreases significantly: from 1130 m/s^2 to 265 m/s^2 when the spool is closed, and from 570 m/s^2 to 170 m/s^2 when the spool is open. These reductions correspond to approximately 76.5% and 70.2%, respectively.

CRediT authorship contribution statement

Linfei Li: Writing – original draft, Investigation, Formal analysis, Data curation. **Yuwen Wang:** Software, Data curation. **Yuchuan Zhu:** Writing – review & editing, Supervision, Resources, Funding acquisition.

Declaration of competing interest

The authors declare that they have no known competing financial interests or personal relationships that could have appeared to influence the work reported in this paper.

Acknowledgements

The authors would like to thank the National Natural Science Foundation of China (NO.52375059) and Jiangsu Province Research and Practice Innovation Program (NO. KYCX24_0554) for providing the funding for this research.

Data availability

Data will be made available on request.

References

[1] Y. Wang, Y. Zhu, J. Ling, et al., Research on the characteristics of sliding valve PHSV, J. Aero. Power 39 (11) (2024) 501–509.
[2] H. Liu, Y. Ruan, Q. Gao, et al., Performance study of adaptive adjustable dual-valtage controller for high speed on/off valve, Chin. Hydraul. Pneum. 48 (11) (2024) 101–110.
[3] X. Yang, X. Hu, F. Xu, et al., Large-range dynamic characteristic adjustment of high-speed on-off valve for water hydraulic manipulators based on multistage voltage and double sliding mode control, Measurement 242 (2024) 116094.
[4] Q Zhong, E Xu, T Jia, et al. Research status and prospect on the control method of high speed on/off valve [J/OL]. J. Mech. Eng., 1-12.
[5] L. Li, Research on High Response Control Strategy of Electromagnetic Screw Cartridge Valve[D], Lanzhou university of technology, 2022.
[6] Z. Liu, L. Li, D. Yue, et al., Dynamic performance improvement of solenoid Screw-In cartridge valve using a new hybrid voltage control, Machines 10 (2) (2022).
[7] Q. Gao, L. Li, Y. Zhu, Hybrid coding control of Electro-hydraulic pressure servo system using array digital valves, J. Mech. Eng. 60 (4) (2024) 143–154.
[8] A. Amini, I. Owen, A practical solution to the problem of noise and vibration in a pressure-reducing valve, Exp. Therm. Fluid Sci. 10 (1) (1995) 136–141.
[9] C. Youn, S. Asano, K. Kawashima, et al., Flow characteristics of pressure reducing valve with radial slit structure for low noise, J. Vis 11 (4) (2008) 357–364.
[10] J. Borg, A. Watanabe, K. Tokuo, Mitigation of noise and vibration in the high-pressure fuel system of a gasoline direct injection engine, Proced. Soc. Behav. Sci. 48 (2012) 3170–3178.
[11] L. Badykova, D. Stadnick, K. Afanasev, et al., Study on Dynamics of Air Pressure Reducing Valve with Focus on the Noise Attenuation Problem[C] Fluid Power Systems Technology, 45820, American Society of Mechanical Engineers, 2014 V001T01A013.
[12] K.S. Peterson, A.G. Stefanopoulou, Extremum seeking control for soft landing of an electromechanical valve actuator, Automatica 40 (6) (2004) 1063–1069.
[13] J. Reuter, S. Maerkl, M. Jaekle, Optimized control strategies for fast switching solenoid valves, Int. J. Fluid Power 11 (3) (2010) 23–33.
[14] J. Tsai, C.R. Koch, M. Saif, et al., Cycle adaptive feedforward approach controllers for an electromagnetic valve actuator, IEEE Trans. Control Syst. Technol. 20 (3) (2011) 738–746.
[15] T. Glück, W. Kemmetmüller, A. Gaeta, et al., Trajectory optimization for soft landing of fast-switching electromagnetic valves, IFAC Proc. Vol. 44 (1) (2011) 11532–11537.
[16] M. Bernardo, S. Santini, A. Kugi, et al., Model-Based soft- Landing Control of an Electromechanical Engine Valve actuator[C]//Dynamic Systems and Control Conference, 45301, American Society of Mechanical Engineers, 2012, pp. 87–94.
[17] P. Mercorelli, A motion-sensorless control for intake valves in combustion engines, IEEE Trans. Ind. Electron. 64 (4) (2016) 3402–3412.
[18] L. Li, Research and Development on Electromechanical Valve Actuation[M], Zhejiang University, Hangzhou, 2004.
[19] R. Huang, Y. Zhao, Soft landing control of electromagnetic valve actuation for engines by using LQR, J. Tsinghua Univ. (Sci. Technol.) (8) (2007) 1338–1342.
[20] C. Deng, Q. Zhan, Sensorless control of high-speed dot-matrix pulse jet generator, Opt Precis. Eng. 20 (4) (2012) 752–759.
[21] X. Zhu, L. Liu, H. Guo, et al., Modeling and analysis of an electromagnetic fully variable valve train with a magnetorheological buffer, Electronics 8 (9) (2019) 996.

[22] H Huang, Z Lei, S Chen, et al. Simulation and experimental analysis of the influence of pressure difference on the noise of high-speed switching valves [J]. J. Mech. Eng., 1-12].
[23] H. Huang, X. Luo, W. Liu, et al., Transient vibration and noise characteristics of on/off valve under high frequency opening and closing, Int. J. Aeroacoustics 24 (3-4) (2025) 195–220.
[24] W Liu. Research on the Fluid-Solid Excitation Source and Vibration Noise Characteristics of Liu Wenli High-Speed Switching Valve [D]. Fuzhou University.
[25] Q Huang. Research on noise evolution law and influencing factors of high-speed On/Off valve for unmanned road sweepers[J]. Chin. Hydraul. Pneum., 48(8): 172-181.
[26] Y. Zhu, Q. Gao, Y. jiang, et al., A soft-landing PWM control method and system for piezoelectric high-speed on-off valves, Jiangsu:CN110594477A (2019) 12–20.
[27] H. Heo, Y. Son, J. Kim, A trapezoidal velocity profile generator for position control using a feedback strategy, Energies 12 (7) (2019) 1222.
[28] H. Li, M.D. Le, Z.M. Gong, et al., Motion profile design to reduce residual vibration of high-speed positioning stages, IEEE ASME Trans. Mechatron. 14 (2) (2009) 264–269.
[29] C Zhang, J Wang, Z Jiang, et al. Research on the impact noise of the main circuit breaker conversion valve of EMU[J]. Mechanical Engineering & Automation, 2022 (4): 4-8.